ECE 416/516
IC Technologies
Lecture 9:
Non-Optical Lithography

Professor James E. Morris
Spring 2012

Chapter 9

Nonoptical Lithographic Techniques

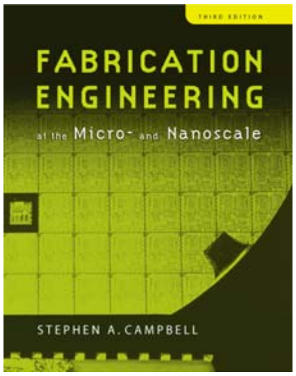

X-Ray Printing System

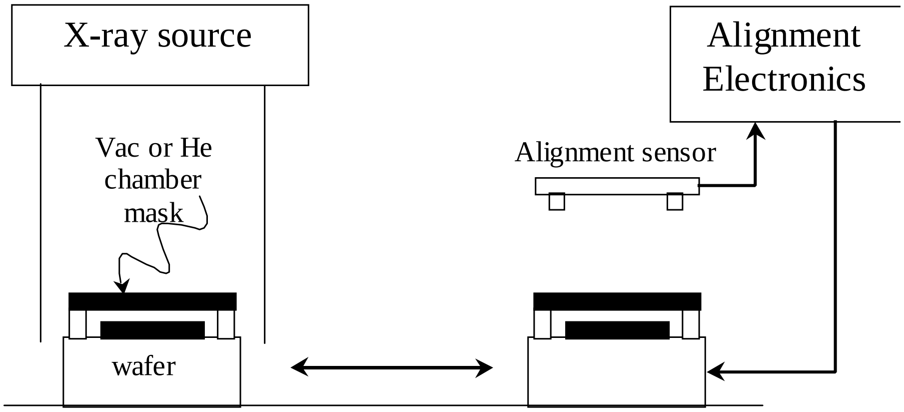

X-Ray Mask materials (Campbell Table 9.2):
Si_3N_4, Si, BN, SiC, W, Au, diamond.
See also: X-Ray generation, X-Ray optics.

X-ray photons: 1-10keV (λ=0.1nm=1Å) → electron-photon interaction

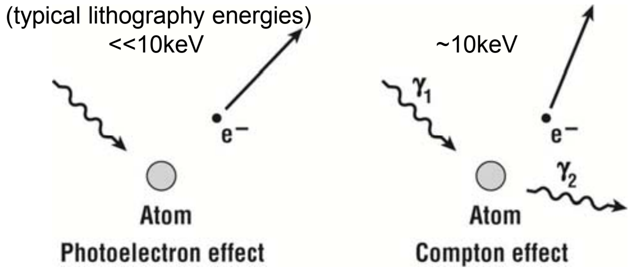

2ndary e^- energies<0.1x e-beam e^- energies
so less energy spread

Absorption $\alpha(\lambda)=\sigma(\lambda)\rho/m$

$\lambda_2-\lambda_1=\lambda_c(1-\cos\theta)$
where λ_c=0.0243Å
and θ=angle between γ_1,γ_2 directions

Figure 9.1 The two dominant interaction processes for high energy photons with matter: the photoelectric effect and Compton scattering.

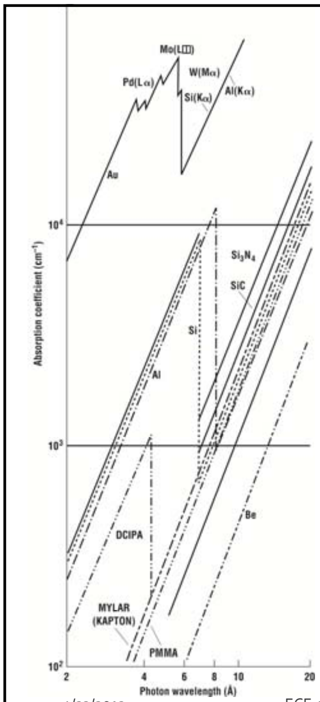

Absorption coefficient α

Low energy, high α
→ need bleaching effects

Discontinuous due to different energy levels

Figure 9.2 Absorption coefficients for some common materials as a function of photon energy *(after Glendenning and Cerrina* [29], *reprinted by permission, Noyes Publications).*

X-Ray Printing Resolution #1

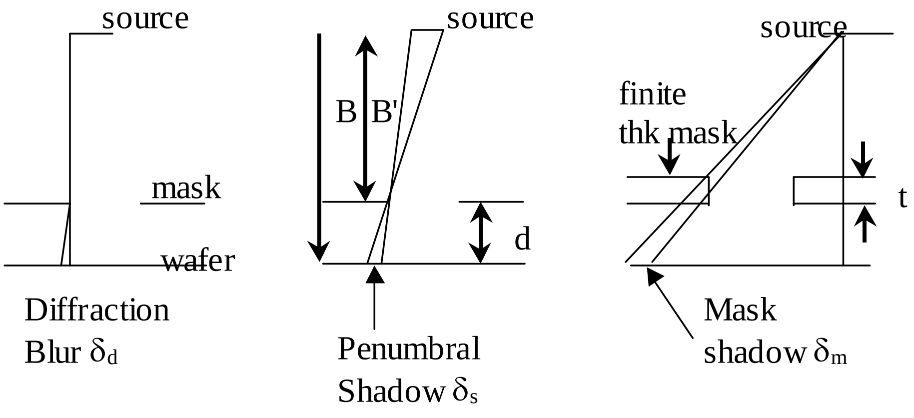

Diffraction
Blur δ_d

Penumbral
Shadow δ_s

Mask
shadow δ_m

X-Ray Printing Resolution #2

Diffraction Blur: $\delta_d = 0.4(\lambda\, d/2)^{1/2}$

Pennubral Shadow: $\delta_S = S_d\, d/B$

where S_d = Source diameter

Mask Shadow: $\delta_m = r\, t / B$

Electron generation in PR: Range $\delta_e = 10^{-23}\lambda^{-7/4}$ (in m)

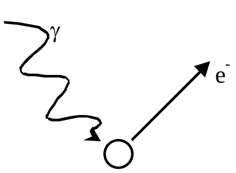

Photo-electric effect

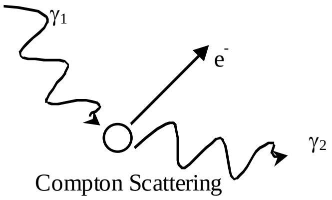

Compton Scattering effect

X-Ray Printing Resolution #3

λ(nm)	δ_d	δ_s	δ_m	δ_e
0.5	40	300	50	190
1.0	57	300	50	56
2.0	80	300	50	17

for: B = 40 cm, d = 40 μm, S_d = 3 mm

r = 20 mm, t = 1 μm

Electron beam lithography (EBL)

Elastic scattering: neutrons (eq'ns 9.3/9.4)

Inelastic scattering: See next slide

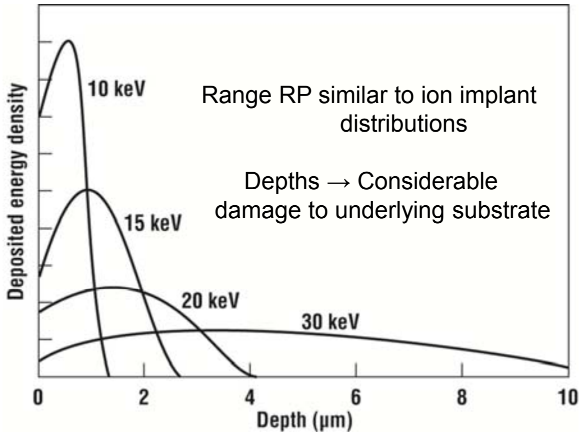

Range RP similar to ion implant distributions

Depths → Considerable damage to underlying substrate

Figure 9.3 Deposited energy density for various energy electron beams incident on silicon as a function of depth.

Inelastic scattering

Monte Carlo simulations, or Bethe equation:

$$\frac{dE}{dx} = \left(\frac{N_A e^4}{2\pi\varepsilon_0^2}\right)\left(Z\frac{\rho}{A}\right)\left(\frac{1}{E}\ln\frac{E}{66J}\right)$$

where N_A =Avogadro's number
Z=atomic number
A=atomic weight
ρ=density
J=mean ionization potential≈11.5ZeV

$$\text{Range } R_P = \int_0^{R_P} dx = \int_{E_0}^{0}\left(\frac{dE}{dx}\right)^{-1} dE$$

Thermionic electron sources

Richardson - Dushman equation

$$J_C = AT^2 \exp - \frac{E_w}{kT}$$

W: 0.5A/cm^2 at 10^{-4}torr
LaB$_6$: 20A/cm^2 at 10^{-6}torr

Brightness β: Collected current

Future:
Zr/W/O field emission: 1000A/cm^2 at 10^{-8}torr with 10nm spot

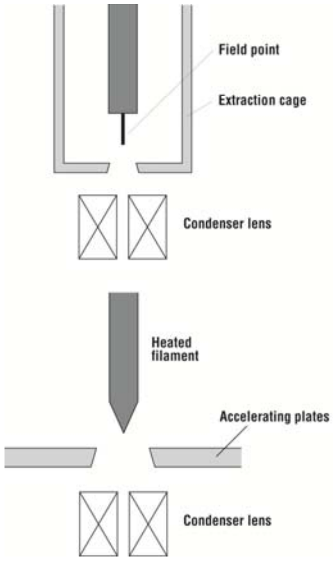

Figure 9.4 Simplified cross section schematics of field emission and thermionic emission electron guns.

Spot diameter: $d^2 = d_0^2 + d_s^2 + d_c^2 \approx d_0^2$

where d_0 due to lens diameter
(source size and space charge)
d_s due to spherical aberration
d_c due to chromatic aberration

Normally:
EBL raster scans
Gaussian beam shape

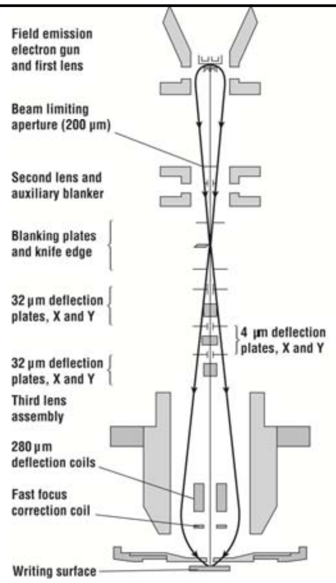

Figure 9.5 System schematic of an early EBES system. The basic column is similar in current generation EBL systems *(after Herriot et al., reprinted by premission, © 1975 IEEE).*

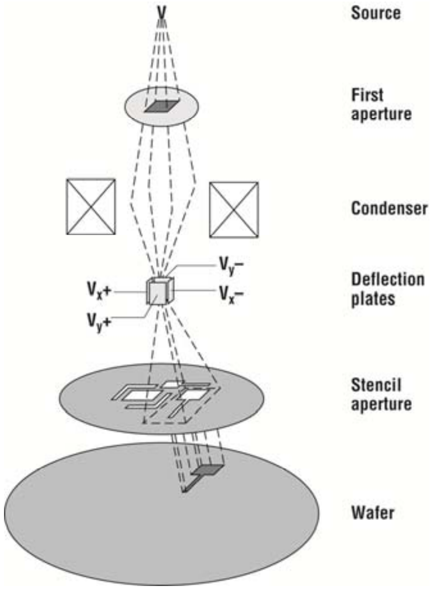

Shaped beams

Sequential rastering limits throughput

e.g. “flat top” from multiple Gaussians

←Multiple pattern replication

plus blank area where EB rastered for special patterns

Figure 9.6 The use of stencil masks with EBL to improve system throughput. This type of exposure is useful only for exposing highly repetitive designs.

Use to expose rectangles of varying size

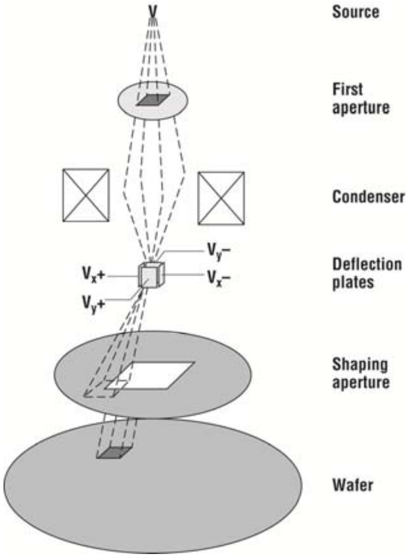

Figure 9.7 A variable shaped beam exposure system using mechanical beam stops for beam shaping. The broad beam exposes many pixels simultaneously, but dimensional control is not as reliable as in standard EBL.

Example

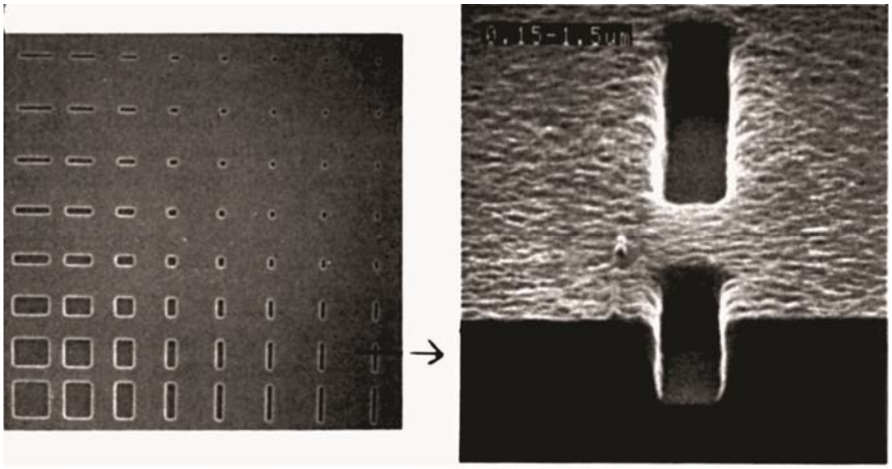

Figure 9.8 Exposure matrix in a variable shaped beam system *(after Hohn, reprinted by permission of SPIE).*

Raster scan Vector scan

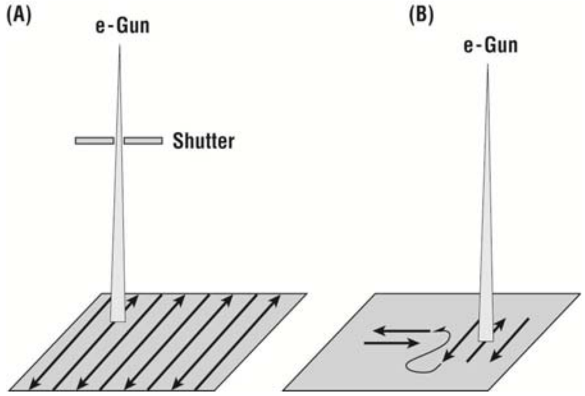

← mechanical →

Figure 9.9 A comparison of scanning methodologies: raster scan (A) and vector scan (B).

EB ~ (0.2-0.5) x min feature size
Multiple scans, beam scan passes every pixel

To minimize scatter broadening, EBL needs a thin resist layer

Double Gaussian exposure distribution:

$$I = I_0\left(\underset{\text{forward}}{e^{-r^2/2\alpha^2}} + \underset{\text{back}}{\eta_E e^{-r^2/2\beta^2}}\right)$$

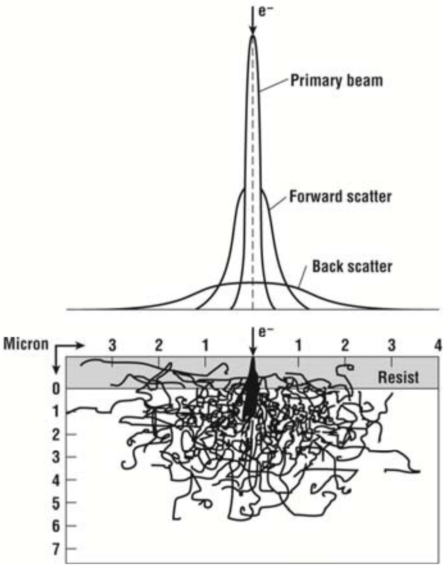

Figure 9.10 Monte Carlo simulation of electron trajectories during an EBL exposure. The upper curve indicates the forward- and backscattered components of the beam *(after Hohn, reprinted by permission, SPIE).*

Proximity effects (forward scattering)

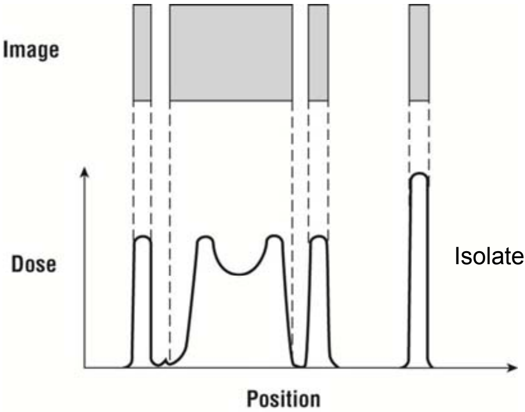

Figure 9.11 Small and large figures to be patterned with EBL requires position-dependent dosage to compensate for proximity effects.

Doses adjusted to account for scattering effects

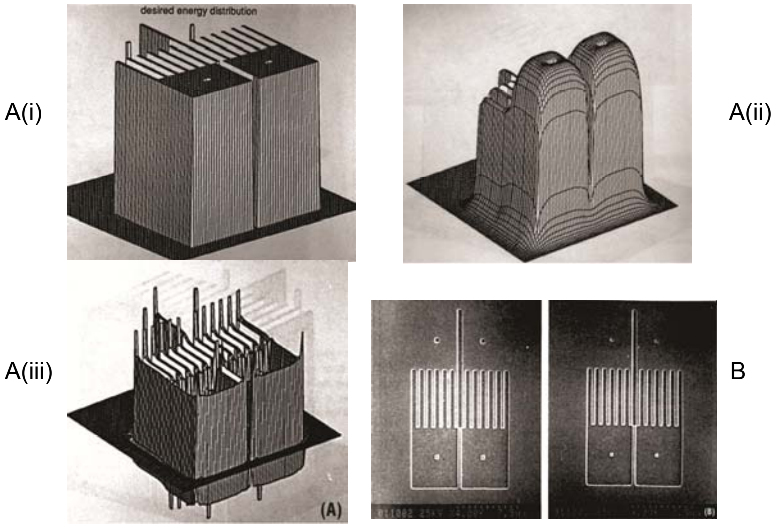

Figure 9.12 (A) Map of (i) desired deposited energy, (ii) uniform dose deposited energy, and (iii) dose map needed to produce a uniform deposited energy; (B) electron micrograph of EBL exposures with and without proximity correction *(reprinted by permission, SPIE, after C.-Y. Chang et al., 1992).*

EBL: 5nm features
Best UV: 50nm features → 22nm node

EBL serial → throughput limited

Figure 9.13 A JEOL-6000FS EBL system *(courtesy of JEOL Corporation).*

Future:

Scanning tunneling microscopy (STM) EBL
(mechanically scanned)

X-Ray

Core levels excited
→ electron returns to core level
→ characteristic energy X-ray photon emitted

Heat → H2O cooled &/or move target

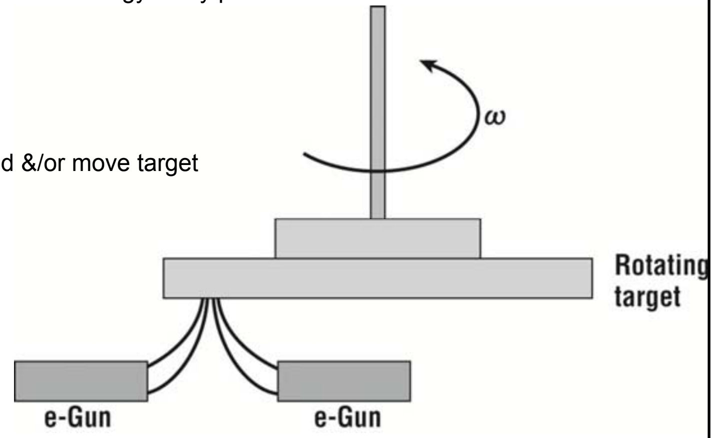

Figure 9.14 A simple rotating electron impact x-ray source uses electron beams focused on a rotating tungsten anode.

Plasma generated X-rays

Heat plasma:
Electron discharge, or
Laser

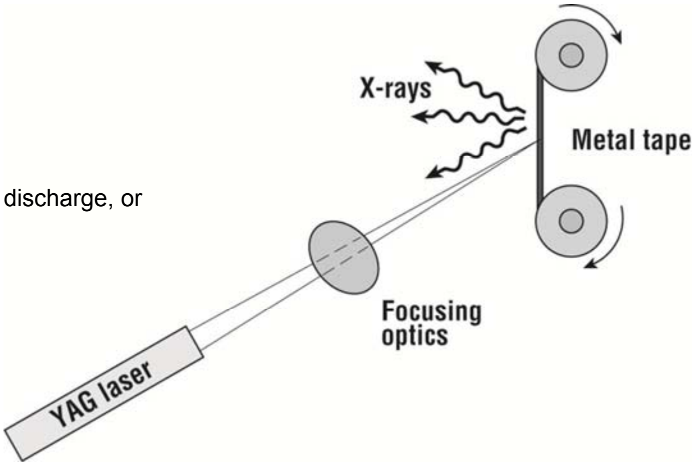

Figure 9.15 Laser plasma-heated x-ray source uses a focused high intensity pulsed laser to ablate a metal film. The superheated metal atoms radiate x-rays.

Synchrotron X-rays

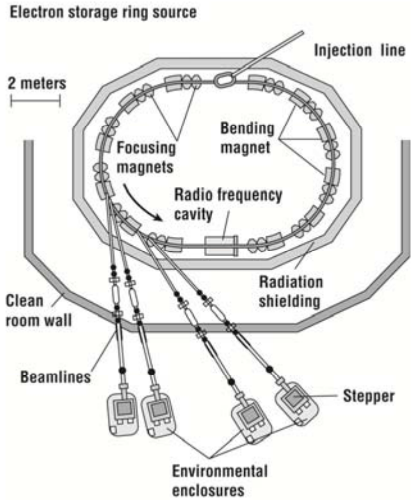

$$E \sim \left(0.3\frac{GeV}{T.m}\right)B.r$$

$$\text{field} \uparrow \uparrow \text{radius}$$

$$\lambda_c(nm) = 0.56\frac{r(m)}{E(GeV)^3} = \frac{1.864}{B(T)E(GeV)^2}$$

$$\sim 1-2nm$$

Figure 9.16 Basic schematic of an electron storage ring for XRL. Several exposure stations are indicated *(after Glendenning and Cerrina, reprinted by permission, Noyes Publications).*

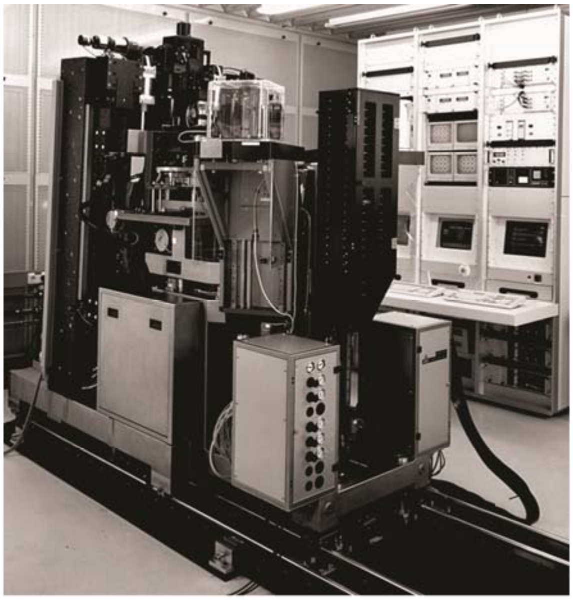

Figure 9.17 Commercial x-ray exposure tool *(courtesy Karl Suss).*

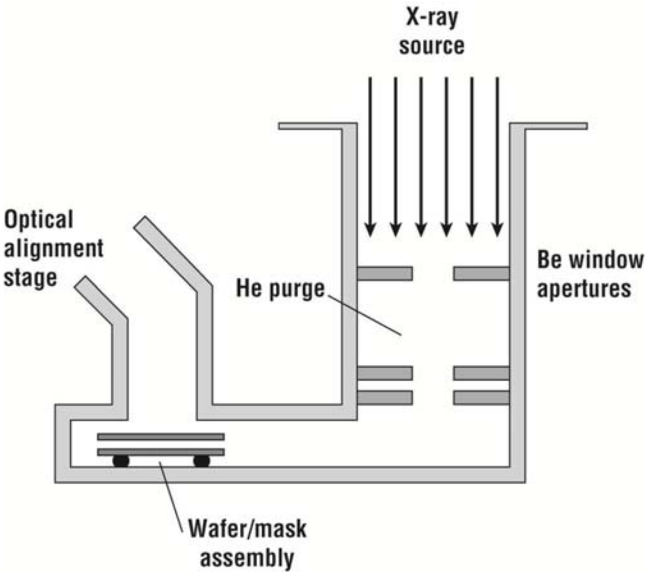

Figure 9.18 Simple proximity x-ray lithography aligner.
The basic system is very similar to optical proximity systems.

1nm photons, features >> λ, so use ray tracing

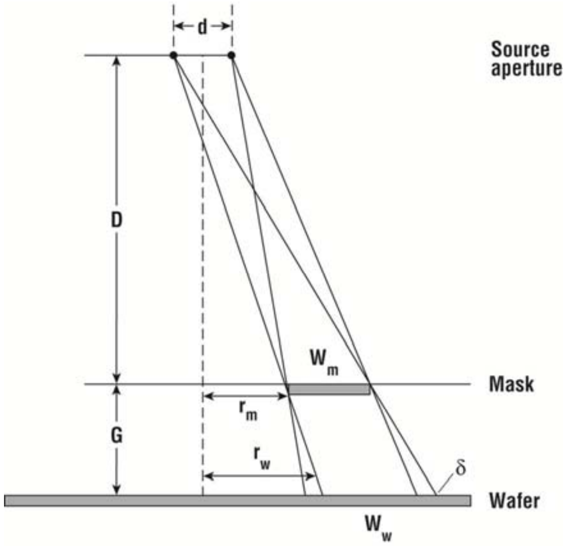

← Problems due to finite size

Pattern distortion:
$R_w = r_m(1+G/D)$

Penumbral blur:
$\delta = G(d/D)$
(resolution)

Figure 9.19 Geometry of the exposure system shown in Figure 9.18.

Reduce distortions by using X-ray lenses

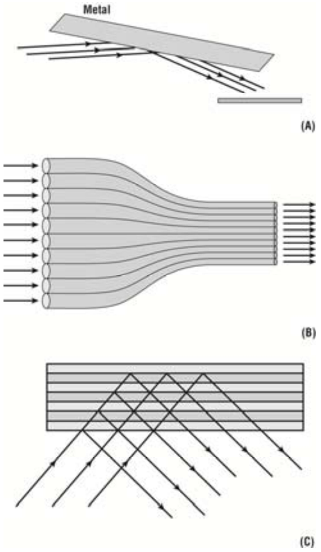

Glass capillary tubes

Alternating layers:
High/low mass
High/low electron concentrations
e.g. Mo/Si
Constructive reinforcement

Figure 9.20 Possible choices for x-ray optics systems include glancing angle metal mirrors (A), Kumakhov lenses (B), and multilayer mirrors (C).

Mask substrate (blank) must transmit X-rays, i.e. low-Z thin film

e.g. Si_3N_4, SiC (Table 9.2)

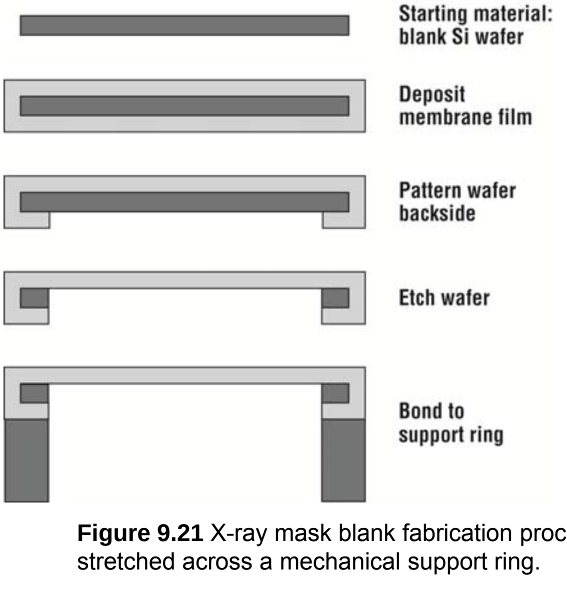

Figure 9.21 X-ray mask blank fabrication process produces a membrane stretched across a mechanical support ring.

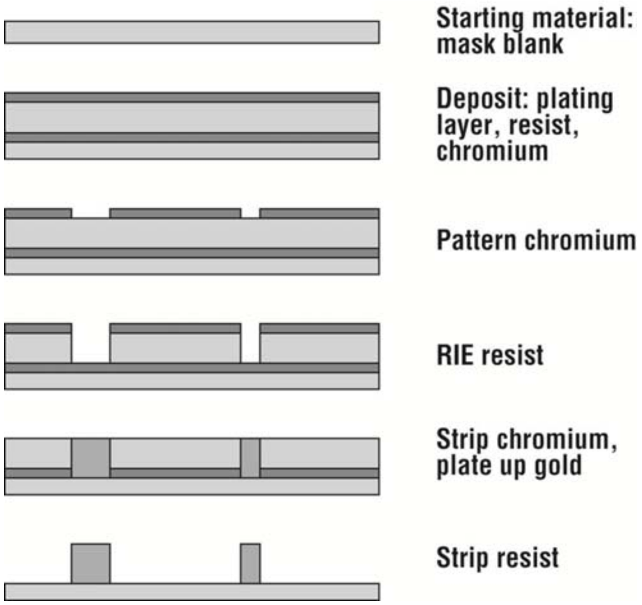

Figure 9.22 Additive process for x-ray mask fabrication.

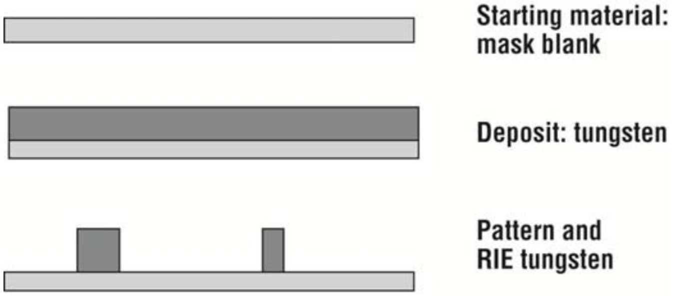

Figure 9.23 Subtractive process for x-ray mask fabrication.

Problem: RIE stop accuracy

Projection X-Ray

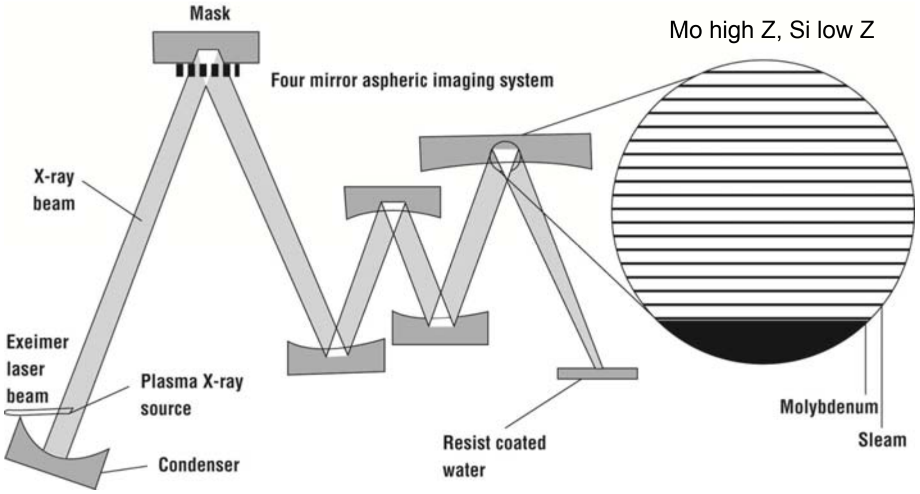

Figure 9.24 An x-ray projection lithography system using x-ray mirrors and a reflective mask *(after Zorpette, reprinted by permission, © 1992 IEEE).*

Projection EBL

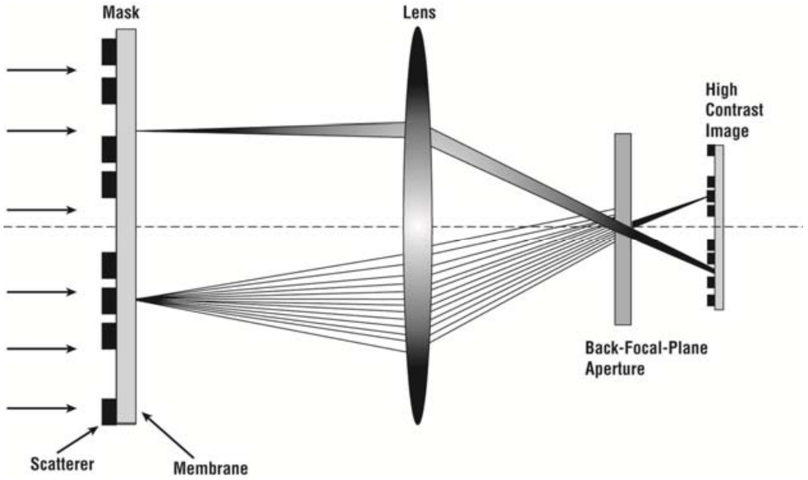

High-Z/Low-Z mask
High Z scatters, doesn't absorb, so heating low

Figure 9.25 SCALPEL principle of operation.

EB and X-ray resists (Table 9.3)

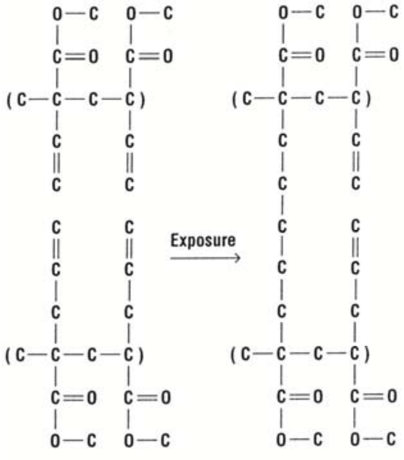

Figure 9.26 Cross-linking of an e-beam resist where the basic PMMA structure has been modified through the addition of a C═C side chain to promote cross-linking.

….. but PMMA scission dominant (Positive resist)

Positive e-beam PR Chemistry

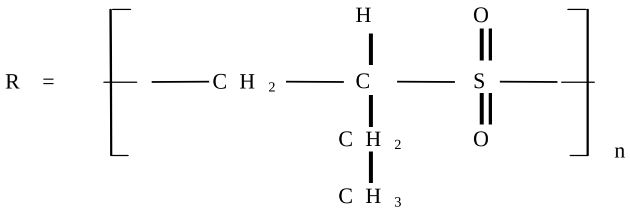

$$R = \left[-CH_2-\overset{\displaystyle H}{\underset{\displaystyle \underset{\displaystyle CH_3}{CH_2}}{C}}-\overset{\displaystyle O}{\underset{\displaystyle O}{\overset{\|}{\underset{\|}{S}}}}- \right]_n$$

Polybutene-1-sulfone

$R = SO_2 - R' \longrightarrow RSO_2^+ +$ ✎R'

$SO_2^+ + R' + R^+$

Radiation --> chain scission & more soluble material

Note: PMMA (polymethyl methacrylate) is similar; radiation --> scission + $CO_2\uparrow$

For negative resists:

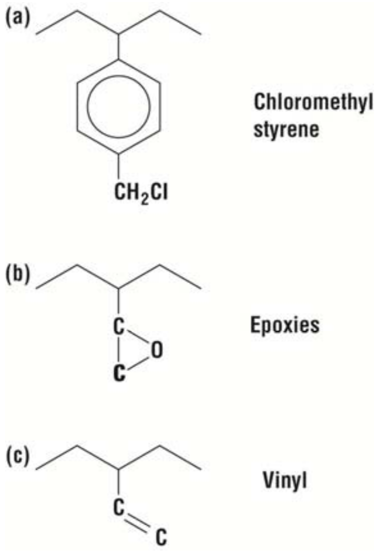

Figure 9.27 Common groups used to promote cross-linking.

EB/X-ray damage to substrate/underlying devices

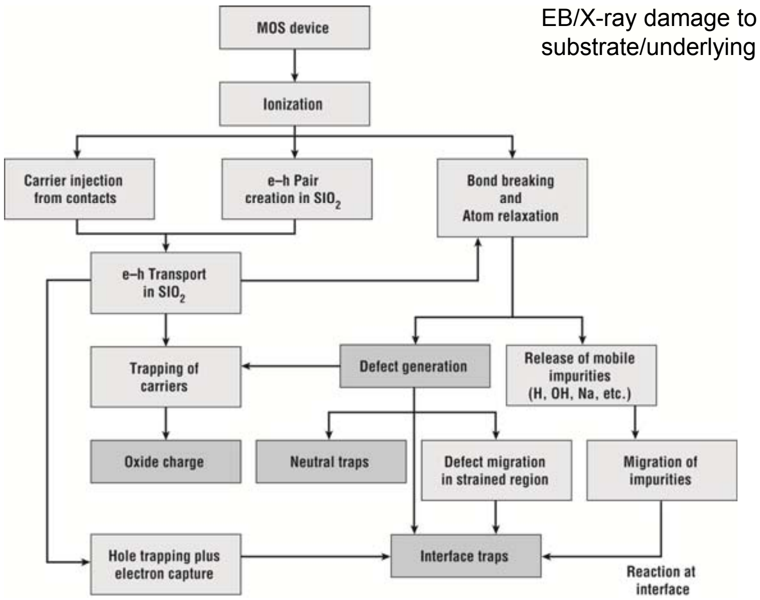

Figure 9.28 Radiation damage flow path *(after Ma and Dressendorfer, reprinted by permission, Wiley).*

Damage example:

Strained Si-Si bond in SiO2 due to O-vacancy → hole capture

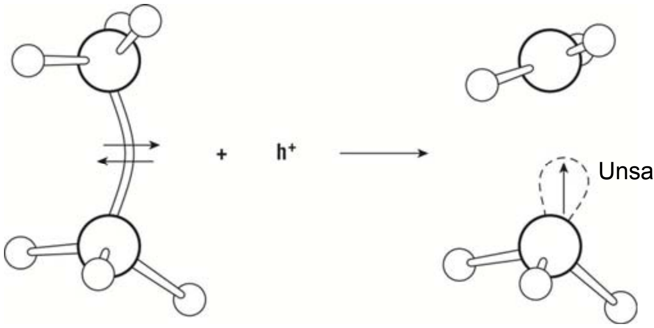

Figure 9.29 An example of a trap creation process believed to occur upon x-ray irradiation of MOS structures. The larger atoms are silicon, the smaller are oxygen. Due to an oxygen vacancy, the two silicon atoms are initially bonded together.

Damage MAY anneal out with later processing (400°C) but some need 700-1000°C

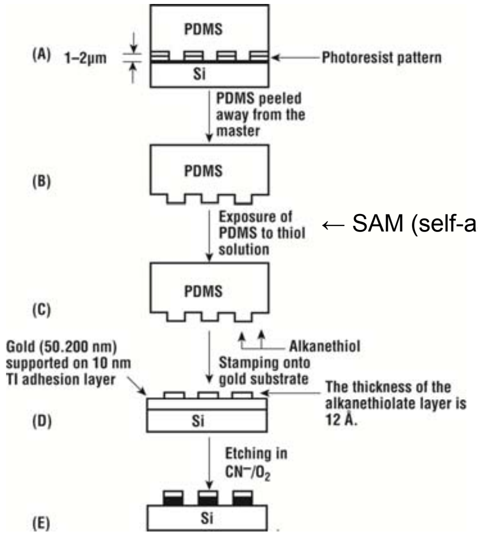

← SAM (self-assembled monolayer)

Figure 9.30 Schematic description for the (µcp fabrication of Au patterns using an elastomer called PDMS (Sylgard 184, Corning): (A) PDMS stamp fabrication, (B) PDMS detach from the master, (C) exposure to the alkanethiol ink, (D) contacting with Au substrate, and (E) etching Au on the substrate *(reprinted with permission from Applied Physics Letters, from Ref. 88.) Copyright 2002, American Institute of Physics.*

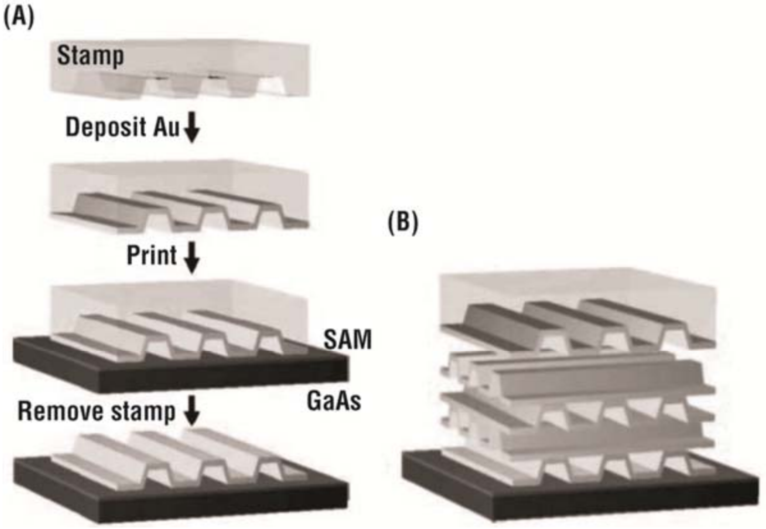

Figure 9.31 Schematic of a 3D micromolding process using a gold layer to form fluid flow channels (reprinted with permission from Nanoletters, from Ref. 92). *Copyright 2003, American Chemical Society.*

PMMA (Tg~100°C) Multiple applications for nanoscale devices

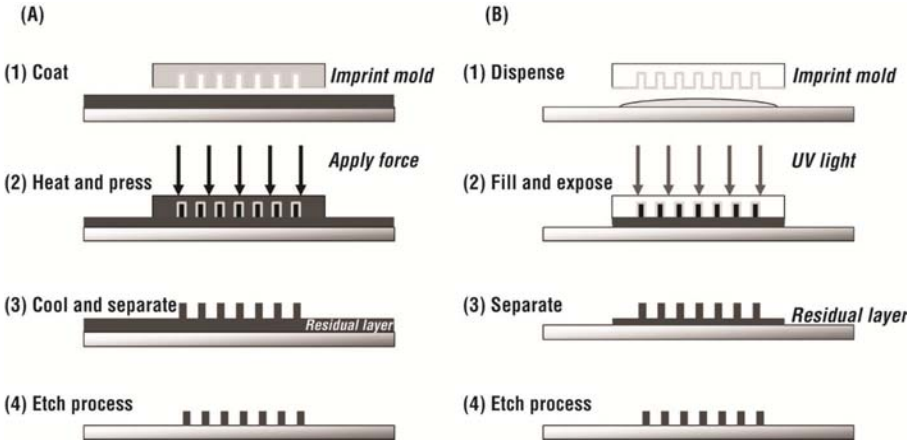

Figure 9.32 Process diagrams for (A) thermal nanoimprint lithography (NIL) and (B) ultraviolet-assisted NIL. In both processes, a mold is pressed into a soft material to form a physical relief image of the mold *(reproduced by permission of the MRS bulletin, from Ref. 103).*

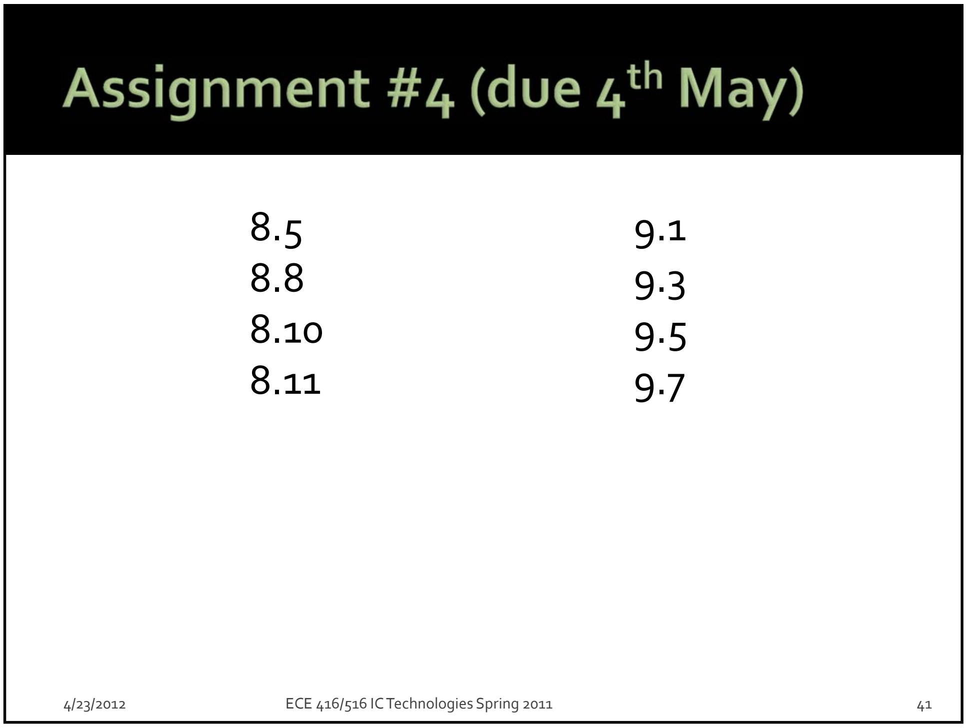

Assignment #4 (due 4th May)

8.5
8.8
8.10
8.11

9.1
9.3
9.5
9.7